



**HAL**  
open science

## Modelling the effect of temperature on phytoplankton growth across the global ocean

Ghjuvan Micaelu Grimaud, Valérie Le Guennec, Sakina-Dorothee Ayata,  
Francis Mairet, Antoine Sciandra, Olivier Bernard

► **To cite this version:**

Ghjuvan Micaelu Grimaud, Valérie Le Guennec, Sakina-Dorothee Ayata, Francis Mairet, Antoine Sciandra, et al.. Modelling the effect of temperature on phytoplankton growth across the global ocean. 8th Vienna International Conference on Mathematical Modelling - MATHMOD 2015, 2015, Vienna, Austria. 10.1016/j.ifacol.2015.05.059 . hal-01245890

**HAL Id: hal-01245890**

**<https://inria.hal.science/hal-01245890>**

Submitted on 17 Dec 2015

**HAL** is a multi-disciplinary open access archive for the deposit and dissemination of scientific research documents, whether they are published or not. The documents may come from teaching and research institutions in France or abroad, or from public or private research centers.

L'archive ouverte pluridisciplinaire **HAL**, est destinée au dépôt et à la diffusion de documents scientifiques de niveau recherche, publiés ou non, émanant des établissements d'enseignement et de recherche français ou étrangers, des laboratoires publics ou privés.

# Modelling the effect of temperature on phytoplankton growth across the global ocean<sup>\*</sup>

Ghjuvan Micaelu GRIMAUD<sup>\*</sup>, Valérie LE GUENNEC<sup>\*,\*\*</sup>  
Sakina-Dorothee AYATA<sup>\*\*,\*\*\*</sup>, Francis MAIRET,<sup>\*</sup>  
Antoine SCIANDRA<sup>\*\*,\*\*\*</sup>, Olivier BERNARD<sup>\*</sup>

<sup>\*</sup> *BIOCORE-INRIA, BP93, 06902 Sophia-Antipolis Cedex, France*

<sup>\*\*</sup> *UPMC Univ Paris 06, UMR 7093, LOV, Observatoire océanologique, F-06234, Villefranche/mer, France*

<sup>\*\*\*</sup> *CNRS, UMR 7093, LOV, Observatoire océanologique, F-06234, Villefranche/mer, France*

---

**Abstract:** : Phytoplankton are ectotherms and are thus directly influenced by temperature. They experience temporal variation in temperature which results in a selection pressure. Using the Adaptive Dynamics theory and an optimization method, we study phytoplankton thermal adaptation (more particularly the evolution of the optimal growth temperature) to temperature fluctuations. We use this method at the scale of global ocean and compare two existing models. We validate our approach by comparing model predictions with experimental data sets from 57 species. Finally, we show that temperature actually drives evolution and that the optimum temperature for phytoplankton growth is strongly linked to thermal amplitude variations.

*Keywords:* phytoplankton, temperature, evolution, Adaptive Dynamics, microalgae, modelling

---

## 1. INTRODUCTION

Phytoplankton gathers planktonic autotrophic organisms, mostly unicellulars, and forms the base of marine food web. Phytoplankton is the input point of inorganic carbon in the trophic net, thanks to photosynthesis. It plays therefore a key role in biogeochemical cycles at global scale (Falkowski et al., 1998). Its activity depends on many factors, primarily light, nutrient availability and temperature (Falkowski and Raven, 2007). In the context of global warming, predicting how the ocean temperature increase will affect marine phytoplankton is a challenging issue.

Several models exist to take into account the direct temperature effect on phytoplankton growth (Eppley, 1972; Geider et al., 1998; Norberg, 2004; Bernard and Rémond, 2012). The models from Eppley (1972) and Norberg (2004) are mostly used in global scale studies (Dutkiewicz et al., 2009; Thomas et al., 2012). However, they assume that the maximum growth rate of a given species ( $\mu_{opt}$ ) increases exponentially with the optimal growth temperature ( $T_{opt}$ ).

We focus here on temperature as an evolution driver in phytoplankton at global scale. Evolution of phytoplankton facing realistic temperature conditions has already been modeled by Thomas et al. (2012) using Norberg (2004) model and by Grimaud et al. (2014) using Bernard and Rémond (2012) model. In line with Thomas et al. (2012) and Grimaud et al. (2014), we use the Adaptive Dynamics theory to study a given temperature-dependent growth

model in an evolutionary perspective. Nevertheless, we propose an original approach based on function optimization which allows to predict the evolutionary outcomes at the global ocean scale. We validate our approach on a data set of 194 observations (extracted from Thomas et al. (2012)) of the temperature response for different species for which isolation sites are known. We compare the different existing models, and we address the questions of how phytoplankton adapts to *in situ* temperature variations, and investigate the implications at global scale. We firstly present a model of the direct temperature effect on phytoplankton growth, we then use it in an evolutionary perspective and finally we compare the results to experimental data.

## 2. MODELLING THE DIRECT EFFECT OF TEMPERATURE ON PHYTOPLANKTON GROWTH

The direct temperature effect on phytoplankton growth is an asymmetric curve with three key parameters, the minimal, optimal, and maximal temperatures for growth ( $T_{min}$ ,  $T_{opt}$ ,  $T_{max}$  respectively) called cardinal temperatures (Fig. 1). The maximal growth rate ( $\mu_{opt}$ ) is defined as the growth rate at  $T_{opt}$ . As a first step, we use the model developed by Bernard and Rémond (2012) based on Rosso et al. (1993) to represent the thermal growth curve (Fig. 1):

$$\mu_B(T) = \begin{cases} 0 & \text{if } T \leq T_{min} \\ \mu_{opt}\phi(T) & \text{if } T_{min} < T < T_{max} \\ 0 & \text{if } T \geq T_{max} \end{cases} \quad (1)$$

with

---

<sup>\*</sup> Corresponding authors ghjuvan.grimaud@inria.fr, valerie.le-guenneec@hotmail.fr

$$\begin{aligned}
\phi(T) &= \frac{\lambda(T)}{\beta(T)} \\
\lambda(T) &= (T - T_{max})(T - T_{min})^2 \\
\beta(T) &= (T_{opt} - T_{min})[(T_{opt} - T_{min})(T - T_{opt}) \\
&\quad - (T_{opt} - T_{max})(T_{opt} + T_{min} - 2T)]
\end{aligned} \tag{2}$$

with

$$T_{opt} > (T_{min} + T_{max})/2 \tag{3}$$

and where  $T$  is the temperature in °C. This model does not make any assumption of structural link between the optimal growth temperature  $T_{opt}$  and the optimal growth rate  $\mu_{opt}$  (an increase of  $T_{opt}$  is not followed by an increase of  $\mu_{opt}$ ). Moreover, the model has only four parameters with biological meanings, which facilitates their estimation with experimental data.

All along this study, we compare Bernard and Rémond (2012) model with Eppley-Norberg temperature model (Eppley, 1972; Norberg, 2004) defined as follow:

$$\mu_E(T) = ae^{bT} \left( 1 - \left( \frac{T - z}{w/2} \right)^2 \right) \tag{4}$$

where  $a$  and  $b$  are parameters without biological meanings ( $a = 0.81$ ,  $b = 0.0631$ ), and  $w$  is the thermal niche width corresponding to  $T_{max} - T_{min}$  in Bernard and Rémond model. Instead of considering the  $T_{opt}$  parameter, this model uses a parameter called  $z$ . It corresponds to the maximum of the quadratic expression of eq. (4) and it is determined by the "Eppley curve"  $T \rightarrow ae^{bT}$  (Eppley, 1972) (Fig. 1 B). However,  $T_{opt}$  can be expressed as a function of  $z$ :

$$T_{opt} = \frac{bz - 1 + \sqrt{(w/2)^2 b^2 + 1}}{b} \tag{5}$$

Using parameter  $z$ , the model assumes that there is a structural link between  $T_{opt}$  and  $\mu_{opt}$ : the higher  $T_{opt}$ , the higher  $\mu_{opt}$ .

Using data sets for 26 species, Grimaud et al. (2014) showed that there exists a linear link between cardinal temperatures:

$$\begin{aligned}
T_{max} &= mT_{opt} + p \\
T_{min} &= rT_{opt} - n
\end{aligned} \tag{6}$$

and with  $m = 0.93$ ,  $p = 9.83$  and  $r = 0.97$ ,  $n = 21.85$ . We thus replaced  $T_{max}$  and  $T_{min}$  in eq.(1) by their function of  $T_{opt}$  in eq.(6). Given the parameter values,  $w$  is almost constant, in accordance with Thomas et al. (2012) approach ( $w = 30$ ). We thus obtain two different temperature models depending only on one parameter  $T_{opt}$ ,  $\mu_B(T, T_{opt})$  and  $\mu_E(T, T_{opt})$ .

### 3. EVOLUTIONARY MODEL FOR THERMAL ADAPTATION

#### 3.1 Slow-fast dynamical system

In line with Grimaud et al. (2014), we include eq.(1) and eq.(4) in a simple chemostat model of phytoplankton growth with varying temperature:

$$M^\epsilon : \begin{cases} \dot{S} = f_S(S, X, T(t)) = D(S_{in} - S) - \mu(T(t))\rho(S)X \\ \dot{X} = f_X(S, X, T(t)) = [\mu(T(t))\rho(S) - D]X \\ \dot{T} = \epsilon f_T(t) = \epsilon \cos(\omega t) \end{cases} \tag{7}$$

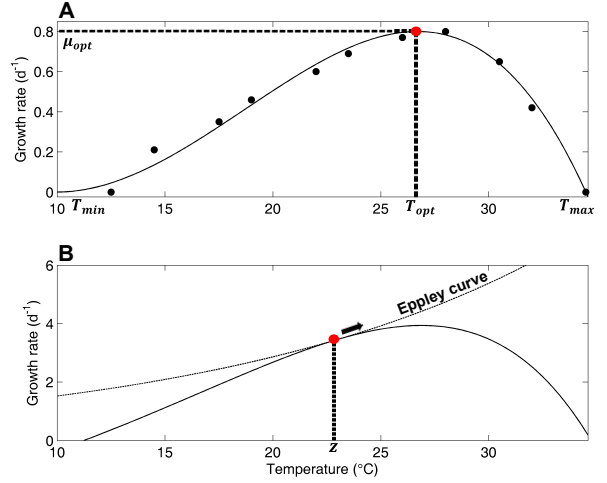


Fig. 1. Thermal growth rate curves using model from Bernard and Rémond (2012) (A) and from Eppley (1972) (B). Both models are calibrated on experimental data from *Synechococcus* strain WH8501 extracted from Thomas et al. (2012), in black circles. However, it is not possible to adjust the maximal growth rate in Eppley (1972) model due to its structural dependence to the "Eppley curve" (dashed line).

$S$  is the nutrient concentration in the chemostat,  $S_{in}$  is the inflow substrate concentration,  $X$  is the algal biomass concentration,  $\mu(T(t))$  is either  $\mu_B(T(t))$  or  $\mu_E(T(t))$ ,  $f_T(t)$  is a periodic function (reflecting seasonality),  $D$  is the dilution rate with  $D < \mu(T(t))\rho(S_{in}) \forall t$ , and  $\rho(S)$  is the substrate uptake defined as:

$$\rho(S) = \frac{S}{K + S} \tag{8}$$

where  $K$  is a half-saturation coefficient. We consider that growth, in term of carbon fixation, is fast compared to temperature fluctuations, *i.e.*  $\epsilon$  is a small positive parameter. It is possible to analyze system ( $M^\epsilon$ ) using the Singular Perturbation Theory (Tikhonov, 1952). The fast dynamics, where  $T(t) = T(0)$ , corresponds to the classical chemostat model:

$$\begin{cases} \dot{S} = f_S(S, X, T(t)) \\ \dot{X} = f_X(S, X, T(t)) \end{cases} \tag{9}$$

System (9) has a unique positive globally asymptotically stable equilibrium  $(S^*(T(t)), X^*(T(t))) \in R_+^2$  (see e.g. Grimaud et al. (2014)), where:

$$S^*(T(t)) = \frac{KD}{\mu(T(t)) - D} \tag{10}$$

$$X^*(T(t)) = (S_{in} - S^*(T(t)))$$

The slow dynamics is given by:

$$M^0 : \begin{cases} S^*(T(t)) = \frac{KD}{\mu(T(t)) - D} \\ X^*(T(t)) = (S_{in} - S^*(T(t))) \\ \dot{T} = \epsilon f_T(t), \quad T(0) = T_0 \end{cases} \tag{11}$$

The reduced system ( $M^0$ ) admits a unique solution  $T^*(t)$ :

$$T^*(t) = T_0 + \frac{\epsilon}{\omega} \sin(\omega t) \quad (12)$$

Tikhonov's theorem (Tikhonov, 1952) allows us to conclude:

*Proposition 1.* For sufficiently small values of  $\epsilon > 0$ , system ( $M^\epsilon$ ) admits a unique positive solution ( $X^\epsilon(t); S^\epsilon(t); T^\epsilon(t)$ ) on  $[0; \tau]$ , where  $0 < \tau < +\infty$ . Moreover:

$$\begin{aligned} \lim_{\epsilon \rightarrow 0} S^\epsilon(t) &= S^*(t) \\ \lim_{\epsilon \rightarrow 0} X^\epsilon(t) &= X^*(t) \end{aligned} \quad (13)$$

From a biological point of view, prop.1 assumes that phytoplankton populations are always at equilibrium because growth is faster than long-term temperature variations. Assuming small annual temperature fluctuation of amplitude  $\delta$ , we obtain  $\epsilon = \delta\omega \ll 1$ . The long-term (*i. e.* annual) dynamics of the algal biomass can thus be approximated by:

$$\begin{aligned} S^*(T(t)) &= \frac{KD}{\mu(T(t)) - D} \\ X^*(T(t)) &= (S_{in} - S^*(T(t))) \\ T(t) &= T_0 + \delta \sin(\omega t) \end{aligned} \quad (14)$$

### 3.2 Evolutionary model using Adaptive Dynamics theory

We study system ( $M^\epsilon$ ) in an evolutionary perspective using the Adaptive Dynamics theory (Dieckmann and Law, 1996). To do so we allow one parameter to evolve, called the adaptive trait, here  $T_{opt}$ . One mutant  $X_{mut}$  appears in the resident population at equilibrium with a different value of  $T_{opt}$ ,  $T_{opt}^{mut}$ :

$$M_{mut}^\epsilon : \begin{cases} S &= S^*(T(t), T_{opt}) \\ X &= X^*(T(t), T_{opt}) \\ \dot{X}_{mut} &= f_{X_{mut}}(T(t), T_{opt}, T_{opt}^{mut}) X_{mut} \\ &= [\mu_{mut}(T(t))\rho(S) - D] X_{mut} \\ \dot{T} &= \epsilon f_T(t) \end{cases} \quad (15)$$

Assuming that the mutant is initially rare, we compute the mutant growth rate in the resident population,  $f_{X_{mut}}(T(t), T_{opt}, T_{opt}^{mut})$ . Depending on the sign of  $f_{X_{mut}}(T(t), T_{opt}, T_{opt}^{mut})$ , the mutant can invade and replace the resident or not. Prop.1 insures that resident population is actually at equilibrium during mutant invasion. Here, because  $T$  is a periodically time varying variable of period  $\tau$ , we use the time average mutant growth rate (Ripa and Dieckmann, 2013):

$$\langle f_{X_{mut}}(T_{opt}, T_{opt}^{mut}) \rangle = \frac{1}{\tau} \int_0^\tau f_{X_{mut}}(T(t), T_{opt}, T_{opt}^{mut}) dt \quad (16)$$

We then compute the selection gradient  $g(T_{opt}, T_{opt}^{mut})$  which gives the selection direction (*e.g.* growing or decreasing values of  $T_{opt}$  are selected through evolution). The selection gradient is defined as the partial derivative of the time average mutant growth rate with respect to  $T_{opt}^{mut}$  evaluated in  $T_{opt}^{mut} = T_{opt}$ :

$$g(T_{opt}, T_{opt}^{mut}) = \left. \frac{\partial \langle f_{X_{mut}}(T_{opt}, T_{opt}^{mut}) \rangle}{\partial T_{opt}^{mut}} \right|_{T_{opt}^{mut} = T_{opt}} \quad (17)$$

At the evolutionary equilibrium, the selection gradient is equal to zero:

$$\left. \frac{\partial \langle f_{X_{mut}}(T_{opt}, T_{opt}^{mut}) \rangle}{\partial T_{opt}^{mut}} \right|_{T_{opt}^{mut} = T_{opt} = T_{opt}^*} = 0 \quad (18)$$

The evolutionary outcome of the model is thus given by the selection gradient. It is possible to simplify the way to find  $T_{opt}^*$ :

*Proposition 2.* The evolutionary equilibrium  $T_{opt}^*$  is given by:

$$T_{opt}^* = \arg \max_{T_{opt}} \langle \ln(\mu(T(t), T_{opt})) \rangle \quad (19)$$

*Proof.* According to Grimaud et al. (2014):

$$\left. \frac{\partial \langle f_{X_{mut}}(T_{opt}, T_{opt}^{mut}) \rangle}{\partial T_{opt}^{mut}} \right|_{T_{opt}^{mut} = T_{opt}} = \frac{D}{\tau} \quad (20)$$

$$\int_0^\tau \frac{\mu'(T(t), T_{opt})}{\mu(T(t), T_{opt})} dt$$

Moreover:

$$\frac{\partial \langle \ln(\mu(T(t), T_{opt})) \rangle}{\partial T_{opt}} = \frac{1}{\tau} \int_0^\tau \frac{\mu'(T(t), T_{opt})}{\mu(T(t), T_{opt})} dt \quad (21)$$

If  $T_{opt} = T_{opt}^*$  (evolutionary equilibrium), eq.(20)=0. Thus:

$$\left. \frac{\partial \langle \ln(\mu(T(t), T_{opt}^*)) \rangle}{\partial T_{opt}} \right|_{T_{opt} = T_{opt}^*} = 0$$

which is equivalent to say that:

$$T_{opt}^* = \arg \max_{T_{opt}} \langle \ln(\mu(T(t), T_{opt})) \rangle$$

## 4. GLOBAL OCEAN SCALE SIMULATIONS

### 4.1 Evolutionary model with realistic temperature signal

We will now study phytoplankton thermal evolution at global ocean scale. Let us consider an ubiquitous phytoplankton species which has evolved locally at each sea surface location ( $i, j$ ) in response to environmental pressure. In a first assumption, each point of latitude/longitude ( $i, j$ ) can be viewed as a chemostat with growth equations given by eq. (7). Assuming that the sea surface temperature is a proxy of the temperature experienced by the phytoplankton cells, we use a realistic temperature signal  $T(t, i, j)$  from *in situ* observations. The sea surface temperature data for the global ocean have been downloaded from the European short term meteorological forecasting website (<http://apps.ecmwf.int>). The data cover the years 2010 to 2012 and the spatial resolution is  $1^\circ$  in latitude and longitude with a temporal resolution of 3 hours.

We calculate for each time step (3 hours) at a given location, the value of the function  $\phi(T(t, i, j), T_{opt})$ , depending on the perceived *in situ* temperature  $T(t, i, j)$  and the optimum growth temperature  $T_{opt}$ . We then calculate the average of the integrated function over  $3\tau = 3$  years (2010, 2011, 2012):

$$\psi(T_{opt}) = \frac{1}{3\tau} \cdot \int_0^{3\tau} \ln(\mu(T(t, i, j), T_{opt})) dt \quad (22)$$

Using prop.2, we search the maximum of eq.(22) and the corresponding  $T_{opt}$  to find the evolutionary optimum temperature  $T_{opt}^*$ .

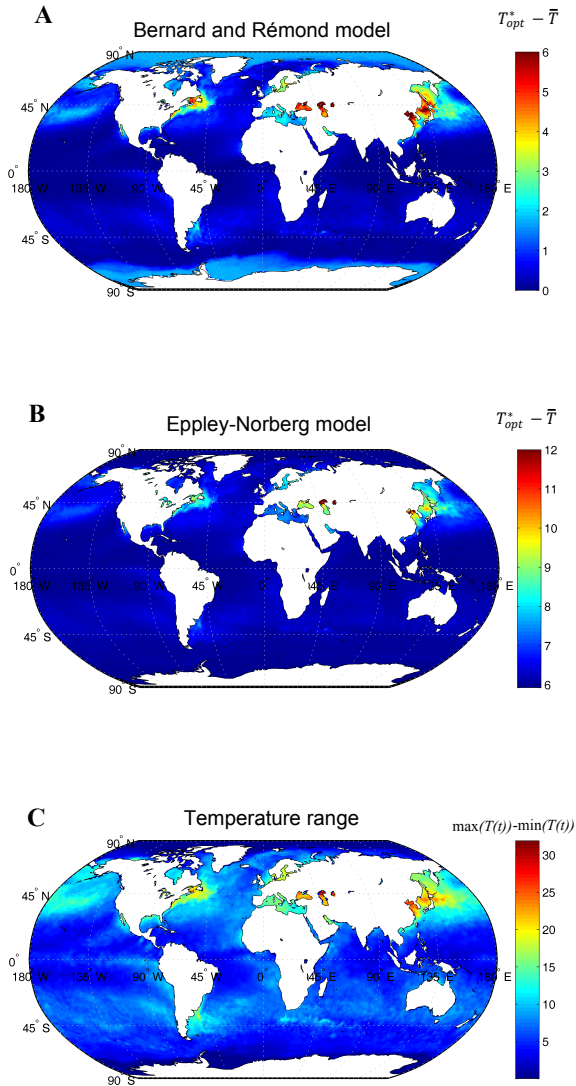


Fig. 2. World map of the difference between the optimal temperature for growth and the mean temperature  $\Delta = T_{opt}^* - \bar{T}$  for Bernard and Rémond model (A) and Eppley-Norberg model (B) (red correspond to areas where  $\Delta \geq 6^\circ\text{C}$  for (A) and  $\Delta \geq 12^\circ\text{C}$  for (B)), and temperature range  $\max(T(t)) - \min(T(t))$  for the three years 2010, 2011, 2012 (C).

#### 4.2 Global scale simulations

Global scale simulations for Bernard and Rémond model (Fig. 2 A) show that for any range of temperature experienced by phytoplankton, the evolutionary temperature  $T_{opt}^*$  at a given place  $(i, j)$  is always higher or equal to the average temperature  $\bar{T}(i, j)$ . In the tropical zone, where the average temperature is high (near  $26^\circ\text{C}$ ),  $T_{opt}^*(i, j) \simeq \bar{T}(i, j)$ . In temperate and coastal zones, where the average temperature is between 10 and  $20^\circ\text{C}$ ,  $T_{opt}^*(i, j) > \bar{T}(i, j)$ . This corresponds to areas where the temperature range  $\max(T(t)) - \min(T(t))$  is higher than  $10^\circ\text{C}$  (Fig. 2 C). We suppose that due to the thermal growth curve asymmetrical

shape, it is more suitable to have higher  $T_{opt}$  when temperature fluctuates. This assumption is in good agreement with Kimura et al. (2013) observations for Archae; these organisms live near their maximum temperature, with a  $T_{opt}$  much higher than the environmental  $\bar{T}$ .

Simulations for the Eppley-Norberg model (Fig. 2 B) show similar results, but the evolutionary temperature is always higher than the average temperature (for about  $6^\circ\text{C}$ ).

#### 4.3 Comparison with experimental data

Using model (1), we determine the cardinal temperatures ( $\hat{T}_{min}$ ,  $\hat{T}_{opt}$ ,  $\hat{T}_{max}$ ) for 194 phytoplankton strains thanks to growth rate versus temperature data sets from Thomas et al. (2012). Because  $\mu_{opt}$  is a function of light and nutrient availability, we normalize the data sets. For each strain, an algorithm developed by Bernard and Rémond (2012) based on the Quasi-Newton Broyden-Fletcher-Goldfarb-Shanno minimizing error method is used to determine the cardinal temperatures. The calibration is coupled to a Jackknife statistical test evaluating the confidence interval of the parameters as in Bernard and Rémond (2012). We then only consider strains associated with data sets providing a confidence interval smaller than  $5^\circ\text{C}$  for the estimated  $\hat{T}_{opt}$ , *i. e.* 57 strains.

Because the geographical coordinates of the isolation of the 194 stains are known, it is possible to compare  $\hat{T}_{opt}$  to *in situ*  $\bar{T}(i, j)$  (Fig. 3 A). Results support the fact that  $T_{opt}$  is much higher than  $\bar{T}$  (here the maximum difference is  $10^\circ\text{C}$ ) in temperate areas and almost the same as  $\bar{T}$  in tropical and polar areas. We simulate the two models at the isolation coordinates of the 57 selected strains (Fig. 3 B, green points). Bernard and Rémond model presents the same non-linear trend previously stated (Fig. 3 B, blue points) whereas Eppley-Norberg model mostly captures a more flattened relationship between  $T_{opt}^*$  and  $\bar{T}$  (Fig. 3 B, red points). For Bernard and Rémond model,  $\Delta$  (defined as  $\Delta = T_{opt}^* - \bar{T}$ ) is always higher or equal to zero due to the assumption that  $\mu_{opt}$  does not depend on  $T_{opt}$ . Because it is observed that  $\Delta$  is nearly equal to zero in tropical zones, this assumption seems justified. Quite the opposite,  $\Delta$  is always higher than  $6^\circ\text{C}$  for Eppley-Norberg model. The linear shape obtained with Eppley-Norberg model plus  $\Delta$  which does not allow to match the points situated in tropical zones are due to the "Eppley curve" hypothesis, which should probably be reparametrised.

We then compare predicted  $T_{opt}^*$  to observed  $\hat{T}_{opt}$  (Fig. 4). For Bernard and Rémond model, mean error calculated as  $|T_{opt}^* - \hat{T}_{opt}|/\hat{T}_{opt}$  is 21.7% whereas for Eppley-Norberg model, mean error is 25.5%. Error is thus quite similar for the two models, but the Eppley-Norberg model overestimates  $T_{opt}^*$  because of its constraint linked to the "Eppley curve". Model predictions are accurate despite some sharp simplifications. Thus, direct temperature effect must drive evolution at global scale, contrary to what is claimed by Marañón et al. (2014).

There are some unavoidable biases in our approach. The first one is due to the age of the cultures which have been used to provide the data. In general, the measurements were not performed right after *in situ* isolation. It results

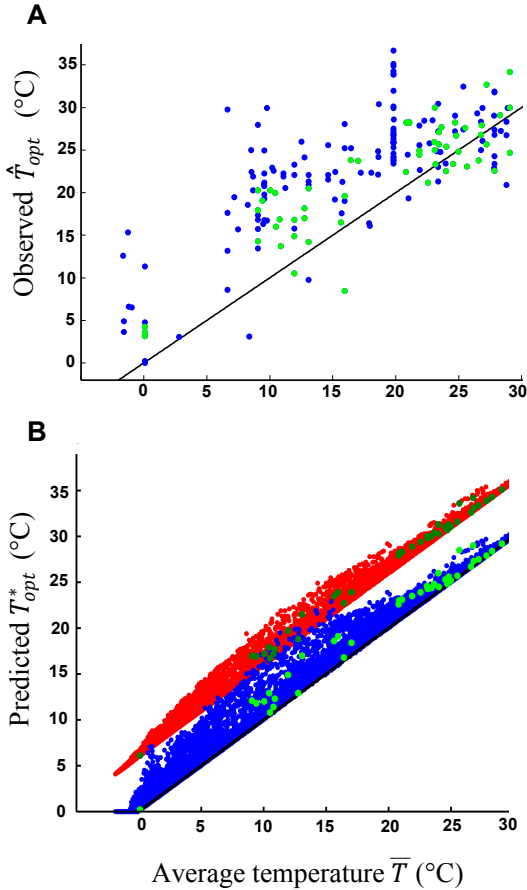


Fig. 3. (A) Observed  $\hat{T}_{opt}$  for 194 phytoplankton strains as a function of  $\bar{T}$ . The 57 selected strains are indicated in green points. (B) Predicted  $T_{opt}^*$  as a function of  $\bar{T}$  for Bernard and Rémond model (blue points) and Eppley-Norberg model (red points). The  $y = x$  curve is indicated in black. The green points correspond to the predicted  $T_{opt}^*$  for the 57 selected strains (light green for Bernard and Rémond model, dark green for Eppley-Norberg model).

that the strains may have evolved, due to the temperature where the strains are stored in the culture collection. Second, we only consider the effect of temperature. Effects of light and nutrients as a master of  $\mu_{opt}$  are not taken into account. Finally, we use sea surface temperature. Phytoplankton can migrate and are advected along the water column, and experience temperatures different from the surface.

Despite these biases, we estimated accurately the  $T_{opt}^*$ , *e.g.* for the cyanobacteria group, which lives in areas where the average temperature is high. It is thus possible that the sea surface temperature, where light is available, is actually a good proxy to predict thermal adaptation.

## 5. CONCLUSION

We have presented a new method based on Adaptive Dynamics theory to study the outcome of phytoplank-

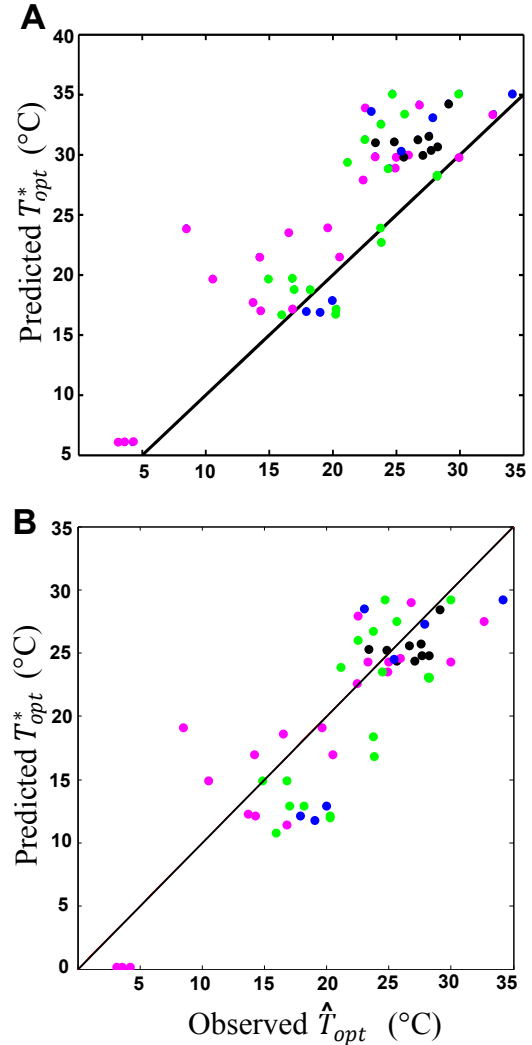


Fig. 4. Predicted  $T_{opt}^*$  compared to experimental  $\hat{T}_{opt}$  for Eppley-Norberg model (A) and Bernard and Rémond model (B). Phytoplankton phylogenetics groups are indicated in color in (B): green, Dinoflagellates, pink, Diatoms, black, Cyanobacteria, blue, others.

ton adaptation at global ocean scale. We defined a standard ubiquitous phytoplankton species and we compared two different thermal growth models describing it in the context of evolution. We found, in agreement with our theory, that the evolutionary optimal temperature  $T_{opt}^*$  is always equal or higher than the average temperature experienced by the phytoplankton  $\bar{T}$ . Moreover, the area with high difference between  $T_{opt}^*$  and  $\bar{T}$  characterizes large temperature fluctuations. When based on Bernard and Rémond, our model successfully fit the data, contrary to the Eppley-Norberg model which linearly link  $T_{opt}^*$  and  $\bar{T}$ , and overestimates  $T_{opt}^*$ . We inferred that direct temperature effect actually drives evolution at the scale of the global ocean. This work is only a first approach to understand thermal adaptation at global scale. The next step will be to study the evolution of the maximum temperature  $T_{max}$  in a context of global warming.

## ACKNOWLEDGEMENTS

This work was supported by the ANR Facteur 4 project. We are grateful to the anonymous reviewers for their helpful suggestions.

## REFERENCES

- Bernard, O. and Rémond, B. (2012). Validation of a simple model accounting for light and temperature effect on microalgal growth. *Bioresource Technology*, 123, 520–527.
- Dieckmann, U. and Law, R. (1996). The dynamical theory of coevolution: A derivation from stochastic ecological processes. *Journal of Mathematical Biology*, 34, 579–612.
- Dutkiewicz, S., Follows, M.J., and Bragg, J.G. (2009). Modeling the coupling of ocean ecology and biogeochemistry. *Global Biogeochemical Cycles*, 23(4).
- Eppley, R.W. (1972). Temperature and phytoplankton growth in the sea. *Fishery Bulletin*, 70, 1063–1085.
- Falkowski, P., Barber, R., and Smetacek, V. (1998). Biogeochemical controls and feedbacks on ocean primary production. *Science*, 281, 200–206.
- Falkowski, P. and Raven, J.A. (2007). Aquatic photosynthesis. *Princeton University Press, New Jersey*.
- Geider, R.J., MacIntyre, K.L., and Kana, T.M. (1998). A dynamic regulatory model of phytoplankton acclimation to light, nutrients, and temperature. *Limnology and Oceanography*, 43, 679–694.
- Grimaud, G.M., Mairet, F., and Bernard, O. (2014). Modelling thermal adaptation in microalgae: an adaptive dynamics point of view. *19th IFAC World Congress, Cape Town (South Africa)*.
- Kimura, H., Mori, K., Yamanaka, T., and Ishibashi, J. (2013). Growth temperatures of archaeal communities can be estimated from the guanine-plus-cytosine contents of 16S rRNA gene fragments. *Environmental microbiology reports*, 5, 468–474.
- Marañón, E., Cermeño, P., Huete-Ortega, M., López-Sandoval, D.C., Mouriño-Carballido, B., and Rodríguez-Ramos, T. (2014). Resource supply overrides temperature as a controlling factor of marine phytoplankton growth. *PloS one*, 9(6), e99312.
- Norberg, J. (2004). Biodiversity and ecosystem functioning: A complex adaptive systems approach. *Limnology and Oceanography*, 49, 1269–1277.
- Ripa, J. and Dieckmann, U. (2013). Mutant invasions and adaptive dynamics in variable environments. *Evolution*, 67, 1279–1290. doi:10.1111/evo.12046.
- Rosso, L., Lobry, J., and Flandrois, J. (1993). An unexpected correlation between cardinal temperatures of microbial growth highlighted by a new model. *Journal of Theoretical Biology*, 162, 447–463.
- Thomas, M., Kremer, C., Klausmeier, C., and Litchman, E. (2012). A global pattern of thermal adaptation in marine phytoplankton. *Science*, 338, 1085–1088.
- Tikhonov, A.N. (1952). Systems of differential equations containing a small parameter multiplying the derivative. *Matematicheskii Sbornik*, 31, 575–586.